Journal of Applied Polymer Science

Heterocoagulation behavior of carbon black with surface encapsulation through emulsion polymerization

Lili Jiang, Wenqi Wang, Aiguo Guan, Guozhang Wu
Shanghai Key Laboratory of Advanced Polymeric Materials School of Materials Science and Engineering, East China University of Science & Technology, Shanghai, 200237, China
Correspondence to: G. Wu (E-mail: wgz@ecust.edu.cn)

ABSTRACT: Nanocomposite microspheres containing styrene–acrylate resin, wax, and carbon black (CB) with desired CB dispersion were prepared through heterocoagulation. The CB surface was modified using conventional anionic emulsifier and anionic dispersants with different lengths of nonionic chains and reactivities or through polymer encapsulation via emulsion polymerization to regulate the dispersion and concentration of CB in the microspheres. Experimental results showed that anionic dispersants with long nonionic chains effectively dispersed and stabilized CB particles. Polystyrene (PS) was then encapsulated on the CB surface by using a reactive dispersant and a water-soluble initiator of polymerization. The CB particles exhibited comparable pH stability with other heterocoagulation components. Overall, encapsulation through emulsion polymerization can be used to obtain not only high CB content but also improved CB distribution in the resulting microspheres. High coagulation efficiency can also be achieved using polystyrene-encapsulated dispersed CB because of its high affinity to emulsifiers and reactive dispersants during dispersion. © 2016 Wiley Periodicals, Inc. J. Appl. Polym. Sci. **2016**, *133*, 43516.

KEYWORDS: emulsion polymerization; nanostructured polymers; surfactants

Received 21 August 2015; accepted 4 February 2016
DOI: 10.1002/app.43516

INTRODUCTION

Nanocomposite microspheres are widely used in coatings, biomedicines, optics, and toners for laser printing.[1–3] Microspheres are conventionally produced through heterocoagulation.[4,5] Temperature, agitation speed, pH, and type and content of coagulants are important factors for controlling heterocoagulation.[6,7] In our previous work[8] on systems containing styrene–acrylate emulsion (Resin), wax particle dispersion (WP), and pigments, we observed a synergistic coagulating effect, in which the coagulation efficiency of each component in the composite was higher than that in the separated state. Further research showed that the pigment particle was the least stable and tended to aggregate earlier than the other components during coagulation when the pH value was changed from basic (pH = 8) to acidic (pH = 2). This phenomenon resulted in poor dispersion and a low content of pigment particles in the microsphere.

Several studies aimed to improve the dispersion stability of inorganic particles by using suitable dispersion method[9] and surfactants,[10–13] introducing *block* or *graft* polymers,[14,15] and encapsulating particles through polymerization.[16–18] Hassan *et al.*[19] prepared high dispersed graphene by sodium dodecyl sulfate (SDS), which assisted adsorption and exfoliation of graphite. Sis and Birinci[20] reported that carbon black (CB) dispersion in aqueous medium became insensitive when the number of the ethylene oxide group was increased by mixing anionic sodium oleate with nonionic surfactants. The stability of inorganic particle[21,22] was also improved using reactive dispersants, such as stearic acid reacting with groups on graphene, which can be adsorbed onto the particle surface through the anchor group, to provide steric stabilization or intensify charges. Morris *et al.*[23] synthesized very high molecular weight copolymer Polyacrylonitrile-co-Maleic anhydride as precursor of carbon fiber, the introduction of copolymer enhanced the tensile properties. Reddy *et al.*[24] reported the modification of multiwall carbon nanotubes and sulfonated polyaniline (MWCNT-SPAN) with alloy nanoparticles embedded by γ radiation, which improved the dispersion in solvents. Multiwall carbon nanotubes (MWCNTs)-core/thiophene polymer-sheath nanocable[25] were synthesized by chemical oxidative polymerization with cationic surfactant, the polymer was deposited on the surface of MWCNTs. In addition to the above, encapsulation of inorganic particles[26–30] by emulsion polymerization has been widely used, which depends on improving the affinity between the nanoparticle and the polymer chain and initiating polymerization on the particle surface. These objectives can be achieved using two methods: induction of initiator adsorption on the particle surface to allow polymerization and the use of reactive dispersants to supply particles with high affinity to the polymer. For example, encapsulation[31] of polystyrene (PS)

or poly(methyl methacrylate) (PMMA) on CB surface through emulsion polymerization effectively prevented surfactant desorption from the CB surface, thereby improving the stability of the dispersion.

Carbon black (CB) has been widely used as a cost-saving black pigment prepared in aqueous dispersions. The pH sensitivity of CB to zeta potential is a key indicator of the stability of colloidal dispersions.[32] In the present work, CB encapsulation was performed through emulsion polymerization by using different types and contents of dispersants, as well as different types of initiators. Variation of zeta potential with pH was determined to obtain the critical coagulation point (CCP) (critical pH value at which the colloid starts coagulating) among styrene–acrylate emulsion (Resin), wax particle dispersion (WP), and CB. To our best knowledge, no published article has investigated the effect of CB pH stability on heterocoagulation of multicomponent microspheres. This study aimed to establish an effective method for controlling the dispersion and concentration of CB in the nanocomposite microspheres.

EXPERIMENTAL

Materials

CB powder (Mogul-L) was purchased from Cabot Corporation (Tian Jin, China) and dispersed in aqueous medium using three anionic dispersants: sodium dodecyl sulfate (SDS,$C_{12}H_{25}SO_4Na$, Sinopharm Chemical, Shanghai, China), alcohol ether carboxylate [Sur-1, $R(CH_2CH_2O)_nCH_2$ CH_2OCOOH, n = 8–10, Sinopharm Chemical, Shanghai, China. "R" represents long alkyl chain], and allyloxy nonyl phenoxy propanol polyoxyethylene ether ammonium sulfonate [SE-10N, $C_{21}H_{33}O_3(CH_2$ $CH_2O)_nSO_3NH_4$, n = 10–20, Ediko, Tokyo, Japan, www.adk.co.jp]. Styrene (St) and butyl acrylate (BA) with a purity of ≥98% were obtained from Shanghai Lingfeng. Ammonium persulfate (APS, ≥99.5%, Aldrich, Shanghai, China) and azobisisobutyronitrile (AIBN, ≥99.5%, Aldrich, Shanghai, China) were used as initiators. Paraffin wax was purchased from shanghai Joule wax Co.

Styrene–butyl acrylate emulsion (Resin, with a particle size of 104 nm and Mw = 13,566, Mw/Mn = 1.80) was synthesized through emulsion polymerization in our laboratory. To control the molecular weight of the polymer, the monomers (110 g styrene, 20 g butyl) were mixed with 2.47 g chain transfer agent (*N*-dodecyl mercaptan, ≥99.5%, Aldrich) to get the monomer mixture. Firstly, seed emulsion containing 0.86 g Sur-1 with 28 mL deionized (DI) water, 13.25 g monomer mixture and 0.21 g APS was obtained after polymerization at 85 °C for 30 min. Simultaneously, 1.75 g Sur-1 with 239 mL DI water was prepared, then 119.22 g monomer mixture and 0.44 g APS were added under stirring to prepare the pre-emulsion. The pre-emulsion was then added dropwise into the seed emulsion for 1 h and reacted at 85 °C for 2 h. The reactor was then immediately cooled in an ice water bath to stop the polymerization. The solid content of the resulting emulsion was 33 wt %, agree well with the theoretical solid content (33.7 wt %).

Paraffin wax dispersion (WP) was prepared using Sur-1 as a surfactant (5 wt % based on the amount of wax) and agitated a homogenizer at 93 °C for 60 min. The aqueous WP dispersion with 25 wt % total solid content was obtained with a particle size of 221 nm.

Table I. The Recipes for Encapsulation of CB Particle by Emulsion Polymerization

Components (g)	St/CB=1/4	St/CB=1/2	St/CB=10/3
CB	4.0	4.0	4.0
Styrene	1.0	2.0	13.3
APS	0.02	0.04	
AIBN			0.27
Denionized water	45	40	145

Preparation and Encapsulation of CB Dispersion through Emulsion Polymerization

Aqueous CB dispersion with 20 wt % total solid content was prepared in a bead mill at 2500 rpm for 50 min, using Sur-1, SE-10N, or SDS (2–5 wt % of CB particles loaded) as a dispersant. Table I lists the composition recipes for encapsulation polymerization. A given amount of St (in the AIBN initiated system, AIBN was directly dissolved in St) was added dropwise to 20 g of CB dispersion. The mixture was diluted with deionized (DI) water to achieve a solid content of 10 wt %. The mixture was then sonicated for approximately 5 min and transferred to a round-bottomed flask mounted in a water bath at 85 °C. After the temperature reached the bath temperature, the mixture was added with 2–4 wt % APS initiator (APS was dissolved in 10 mL DI water) and then stirred at 200 rpm for 2 h. The mixture was further heated to 88 °C for 1 h and the reaction was terminated by cooling to room temperature.

Preparation of Nanocomposite Microspheres through Coagulation

CB, Resin, and WP dispersions (the solid weight ratio of CB/Resin/WP = 10/84/6) were mixed with 300 mL DI water to obtain 10 wt % total solid content and then were loaded into a 1000 mL reactor. After stirring for 15 min, the mixture was added with H_2SO_4 (2.5 wt %) until the pH approached 2.0–2.1 under agitation by a three-blade marine type propeller agitator at 1200 rpm to initiate the heterocoagulation. The mixture was then heated to 65 °C and maintained for 2 h to ensure completing of the coagulation process. Next, the pH of the mixture was adjusted to 7.0–7.5 by adding NaOH (1.0 wt % water solution). The mixture was finally transferred to an autoclave and kept low speedy (300 rpm) stirring at 130 °C for 2.5 h to generate completely fused microspheres.

The obtained microspheres were thoroughly washed with DI water to remove emulsifiers and residual dispersants on the surface. The microspheres were then dried in a vacuum oven at 40 °C for 48 h to remove water prior to characterization.

Characterization

The weight average molar mass (Mw) and polydispersity (PDI) (Mw/Mn) of Styrene–butyl acrylate emulsion were measured by Gel Permeation Chromatography (GPC, Waters 1515). The emulsion was thoroughly washed with DI water to remove emulsifiers and then dried in a vacuum oven at 40 °C for 48 h

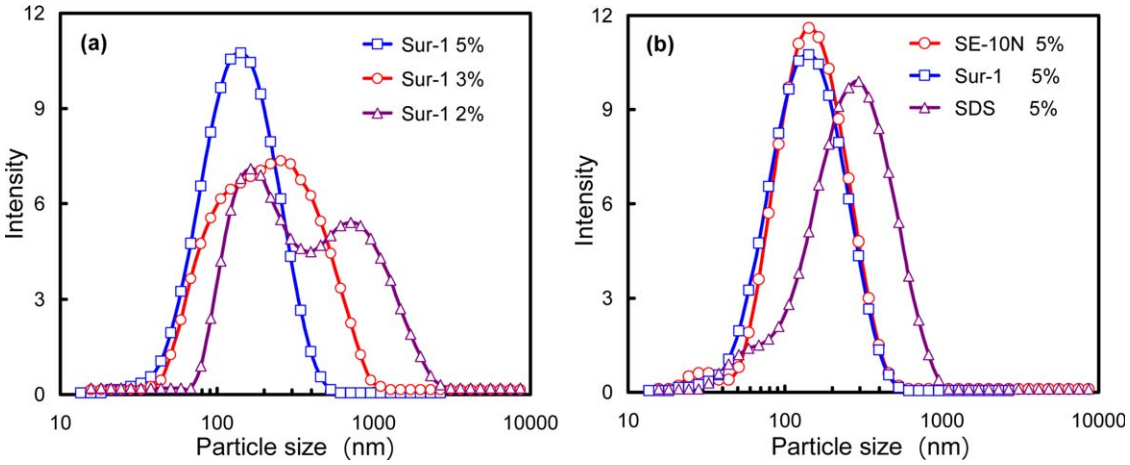

Figure 1. Particle size of CB dispersion by DLS, effect of (a) amount of Sur-1 and (b) different dispersant with same amount on the dispersion of CB. [Color figure can be viewed in the online issue, which is available at wileyonlinelibrary.com.]

to remove water prior to characterization. About 2 mg resin powder was dissolved in 1 mL N, N-Dimethylformamide (DMF) and stirred to ensure complete dissolution. Then the Mw and PDI were obtained.

The particle size and zeta potential of CB, Resin, and WP aqueous dispersions were measured by dynamic light scattering (DLS, Malvern Mastersiser Nano-ZS90). A drop of aqueous dispersion was diluted 1000 times with DI water. For zeta potential measurement, the pH of the sample was adjusted by adding 2.5 wt % H_2SO_4. The measurement was repeated three times and the average zeta potential was obtained.

Morphology observation was conducted through transmission electron microscopy (TEM, Hitachi, JEM-1400) at an accelerating voltage of 100 kV. A drop of aqueous dispersion was diluted 10 times with DI water, dropped to a copper net, and dried with an infrared lamp to observe CB particles in the dispersion. The microspheres were embedded in a cured epoxy resin and then cut into sections with 60–90 nm thickness by an ultramicrotome. Scanning electron microscopy (Hitachi, S-4800) was then employed to observe the distribution of microspheres in the aqueous medium.

Fourier transform infrared spectra (FTIR) were obtained using a Nicolet 5700 IR spectrometer at room temperature through the potassium bromide (KBr) pellet method. The FTIR spectra of all the samples were recorded from 4000 cm^{-1} to 500 cm^{-1}, with 64 scans at a resolution of 0.9 cm^{-1}.

Differential scanning calorimetry (DSC, TA Instruments Q800) was performed under purging with dry nitrogen at a flow rate of 40 mL/min. Approximately 5–10 mg of the samples were first heated to 150 °C at 10 °C/min, maintained at 150 °C for 5 min, and then cooled to 0 °C to eliminate thermal history. The samples were subsequently reheated to 150 °C at 10 °C/min to check the glass transition temperature of the encapsulated polymer. Emulsifiers and dispersants were removed by washing in DI water to determine the amount of wax in the microspheres. A characteristic melting peak of wax appeared in the second heating curve near 84 °C. The amount of wax, namely, ω(WP), can be calculated using melting enthalpy (H) with the following equation:

$$\omega(\mathrm{WP}) = k\frac{H}{H_0} \times 100\%$$

where H_0 is the melting enthalpy of pure wax (121 J/g) and k (0.85) is a constant related to cooling rate and sample cell of DSC.

Thermogravimetric analysis (TGA, Netzsu) was performed under purging with nitrogen gas at a flow rate of 20 mL/min and a heating rate of 10 °C/min from room temperature to 1000 °C.

RESULTS AND DISCUSSION

Preparation of CB Dispersions: Effect of Dispersant

Figure 1 shows the particle size distribution of CB dispersion added with different types and amounts of anionic dispersants at a fixed solid content of 20 wt %. As the amount of the dispersant increases from 2 wt % to 5 wt %, CB dispersion exhibits small particle size and narrow particle size distribution. At 5 wt % Sur-1, the particle size of CB dispersion decreases to 144 nm and the polydispersity index (PDI) reaches 0.211 [Figure 1(a)]. Similar to that in Sur-1, CB dispersed with SE-10N exhibits excellent stability (particle size = 141 nm, PDI = 0.224). By contrast, CB does not easily disperse in SDS (particle size = 294 nm, PDI = 0.357; Figure 1(b)).

The results of laser particle size analysis are confirmed by TEM observation. As shown in the TEM images in Figure 2, SDS–CB dispersion contains larger amount of big aggregates than that of Sur-1-CB dispersion, whereas CB in SE-10N exhibit good dispersion. Accordingly, anionic compounds with long nonionic chains added with same amount of dispersant effectively disperse the CB agglomerations.

Encapsulation of CB through Emulsion Polymerization

Based on the results of previous studies, CB dispersion stabilized by the reactive dispersant SE-10N was used for emulsion polymerization, with St as the monomer. APS is a kind of water-soluble initiator, while AIBN is oil soluble. APS initiated emulsion polymerization is based on micelle nucleation mechanism, while in AIBN initiated system, droplet nucleation plays the major role. To distinguish the effect of initiation mechanism on CB encapsulation, AIBN and APS were used in this study.

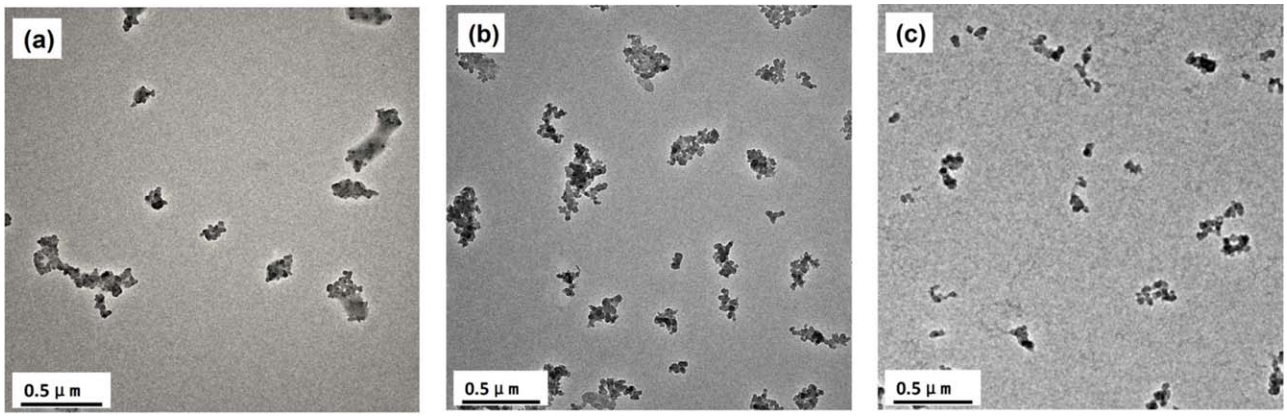

Figure 2. TEM micrographs of CB dispersion with (a) Sur-1, (b) SDS, and (c) SE-10N as dispersant. [Color figure can be viewed in the online issue, which is available at wileyonlinelibrary.com.]

CB encapsulation was performed at a given mass ratio of St to CB (St/CB = 10/3), with AIBN as the initiator. As shown in Figure 3(b,c), large amounts of polymer latex with a particle size of 90 nm are observed in the aqueous dispersion, which is a little larger than the emulsion polymerized without CB [50–60 nm in Figure 3(a)]. In presence of CB, CB tends to capture free radicals leading to the reduction of the concentration of initiator. Consequently, the particle size of the latex particle tends to become larger. The latex is not adsorbed on the CB surface and does not contain encapsulated CB particles. The TGA results of CB dispersions before and after centrifugation (8000 rpm (3578 × g) for 10 min) are shown in Figure 3(d). The content of organic

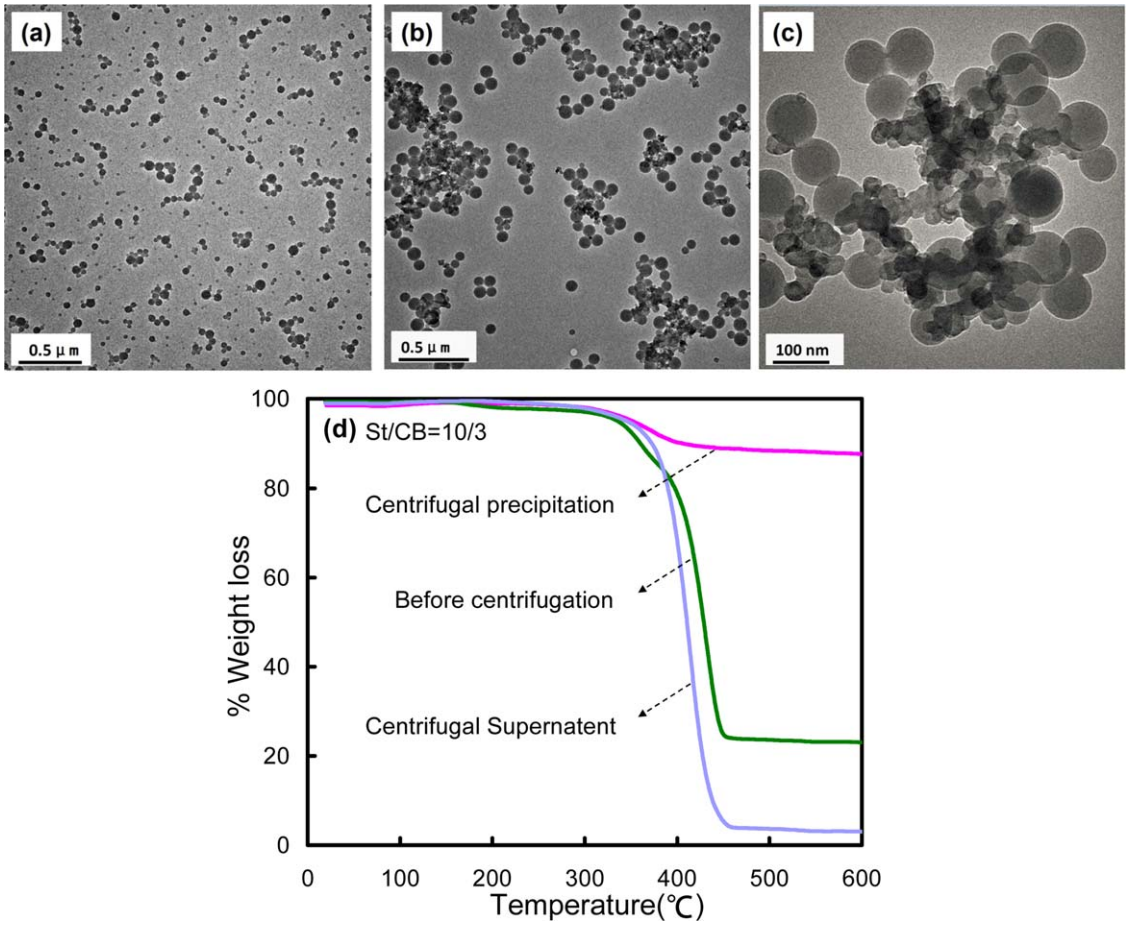

Figure 3. Encapsulation of CB using AIBN as initiator. TEM micrographs of (a) Emulsion polymer without CB, (b,c) encapsulation of CB with styrene with different amplification, and (d) TGA curves before and after centrifugation. (The mass ration of St to CB is 10:3). [Color figure can be viewed in the online issue, which is available at wileyonlinelibrary.com.]

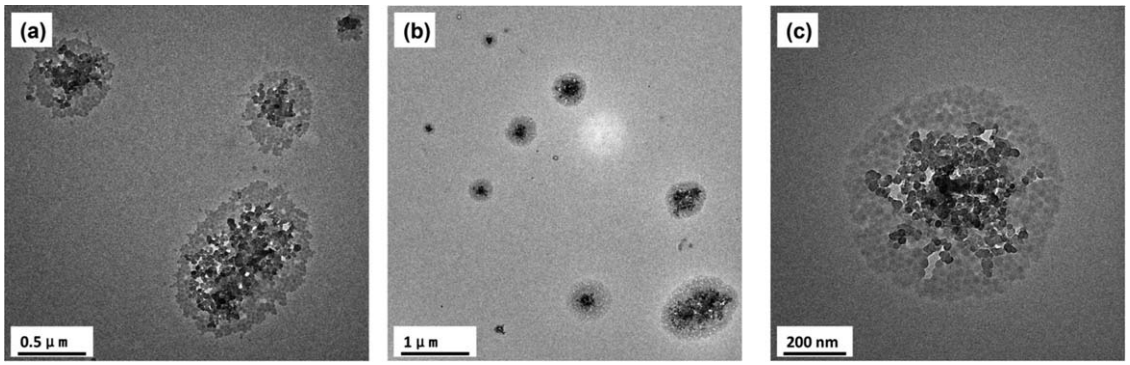

Figure 4. TEM micrographs of encapsulated CB particles with different mass ratios. (a) St/CB= 1/4, (b) and (c) St/CB= 1/2 with different amplifications.

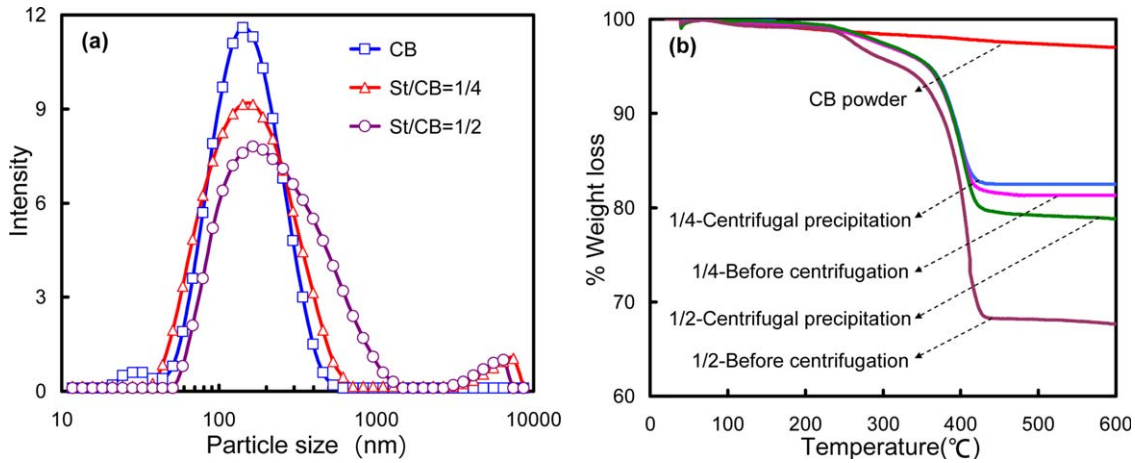

Figure 5. (a) Particle size distribution and (b) TGA curves before and after centrifugation of encapsulated CB particles using APS as initiator. [Color figure can be viewed in the online issue, which is available at wileyonlinelibrary.com.]

compounds before centrifugation is 76.5 wt %, which approximates the feed level of St (76.9 wt %). After centrifugation, the content of precipitated organic compounds is only 12.4 wt %, whereas that of residuals in the dispersion state reaches 97.9%. Similar results are observed for emulsion polymerization with different St/CB ratios. Hence, the polymer latex can be separated from CB particles and the use of AIBN as polymerizing initiator cannot lead to suitable encapsulation of PS on the CB surface.

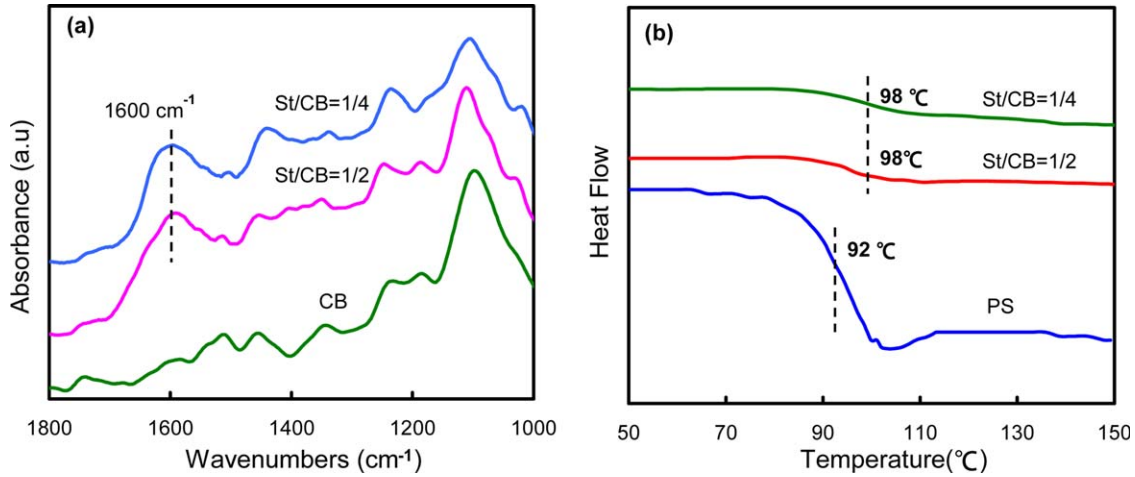

Figure 6. (a) FTIR spectra and (b) DSC curves of the encapsulated CB particles using APS as initiator. [Color figure can be viewed in the online issue, which is available at wileyonlinelibrary.com.]

Table II. Particle Size and CCP of Resin, Wax, and CB Dispersions in the Heterocoagulation

Sample	Dispersant/ emulsifier	Particle size (nm)	CCP
Resin	Sur-1	104	2.5
Wax	Sur-1	221	2.2
1# CB dispersion	Sur-1	140	5.0
2# CB dispersion	SE-10N	141	2.2
3# CB dispersion	SE-10N + PS encapsulated	170	2.0
4# CB dispersion	SE-10N + PS encapsulated	190	1.8

In contrast to AIBN, which can only be dissolved in St, the initiator APS is soluble in water. Figure 4(a,b) show the TEM images of the precipitates after centrifugation of emulsion-polymerized CB dispersions with different ratios of St to CB (1:4 and 1:2). A polymer layer is apparent around the CB particle and the polymer layer of the encapsulation system with St/CB = 1/4 is slightly thinner than that of the other system with St/CB = 1/2. The DLS spectra in Figure 5(a) illustrate the particle size distribution of CB dispersions. The particle size of the encapsulated sample with St/CB = 1/4 is 170 nm, whereas the other system with St/CB = 1/2 is 190 nm, which are both larger than the CB dispersion (particle size = 141 nm) before encapsulation.

TGA was performed to confirm the encapsulation of PS on the CB surface [Figure 5(b)]. As shown, water and the other impurity are evaporated below 200 °C, and when the temperature is higher than 200 °C, polymers with lower molecular weight start to degrade. The organic compounds seem to degrade completely at temperatures above 450 °C and the left compound should be CB particles. The organic compound content of precipitates obtained from centrifugation in the St/CB = 1/4 system is 17.5 wt %, which approximates the feed level of St (20 wt %). This finding implies the high encapsulation efficiency of the system. However, in the St/CB = 1/2 system, the content of organic compounds is 21.2 wt %, which is lower than the feed value (33.3 wt %). This finding suggests that large amounts of St generate numerous free latex particles. In addition, the FTIR spectra in Figure 6(a) shows the existence of sharp peak at 1100 cm^{-1}, 1250 cm^{-1}, and 1450 cm^{-1} both in pure CB sample and PS-encapsulated CB, which represent the C–H and C–C stretching in alkyl groups. Meanwhile, a characteristic peak of C = C stretching in benzene ring at 1600 cm^{-1} appeared in the PS-encapsulated CB, which provide clear evidence of the presence of PS on the CB surface. Moreover, DSC results in Figure 6(b) reveal that both samples exhibit a glass transition temperature at approximately 98 °C, which is slightly higher than that of the neat PS (about 92 °C); hence, PS surrounding the CB surface has high molecular weight and strongly absorbed by the CB surface.

Variation of Zeta Potential with pH for Different CB Dispersions

The stabilities of different CB dispersions with varied pH were investigated. As illustrated in Table II, Samples 1# and 2# represent CB dispersions with 5 wt % Sur-1 and 5 wt % SE-10N as dispersant, respectively. Meanwhile, Samples 3# and 4# denote CB dispersions encapsulated with PS through emulsion polymerization for the St/CB = 1/4 and St/CB = 1/2 systems, respectively. At zeta potential lower than 30 mV, the dispersion is unstable and favorable for coagulation. Therefore, the pH at which the zeta potential decreases to 30 mV is defined as the critical coagulation point (CCP) in this study.

Figure 7 presents the variation of zeta potential with pH value for Resin, WP, and CB dispersions. The zeta potentials of Resin and WP are high under neutral condition and decrease as pH decreases, with CCPs of 2.5 and 2.2, respectively. The high dispersion stability of Resin and WP dispersions could be ascribed to their organic nature. By contrast, CB dispersed with Sur-1 (Sample 1#) is less stable than Resin and WP, with a zeta potential of −35 mV at pH 7 and CCP of 5.0 [Figure 7(a)]. Sample

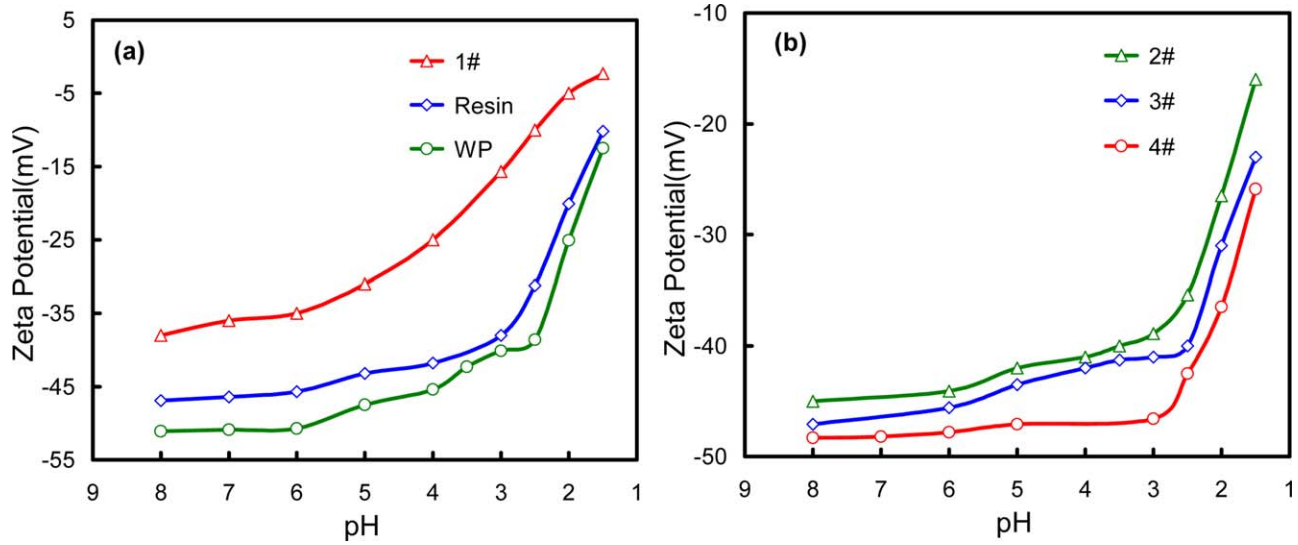

Figure 7. Zeta potential of different dispersions at various pH, (a) Resin, wax, and 1# CB dispersion (b) 2#, 3#, and 4# CB dispersion. (The number of the CB dispersion is shown in Table II and the article.). [Color figure can be viewed in the online issue, which is available at wileyonlinelibrary.com.]

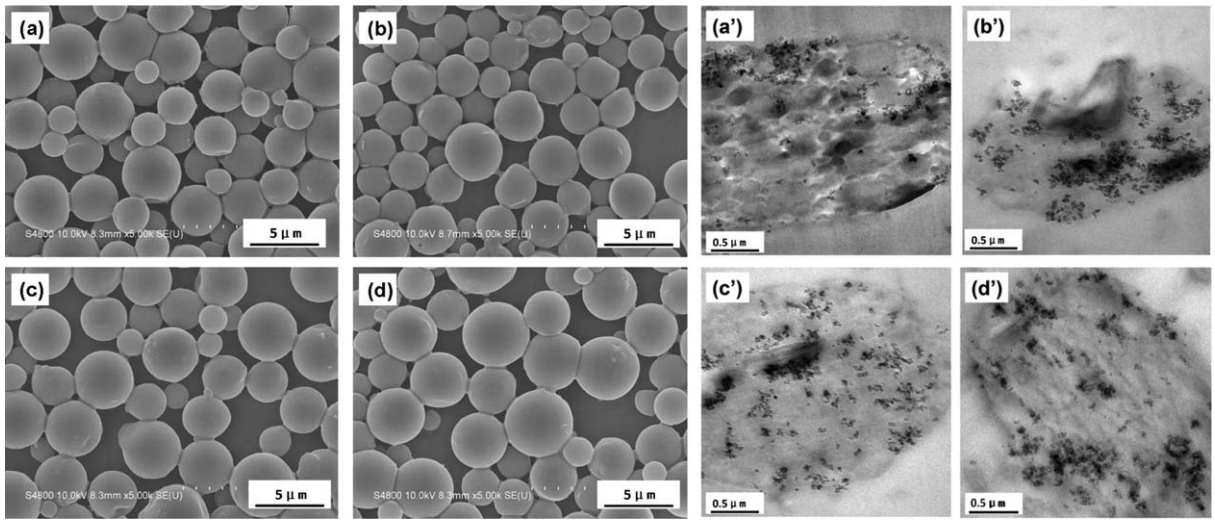

Figure 8. (a–d) SEM photographs and (a'–d') TEM micrographs of microspheres with different CB dispersions, (a) and (a') 1# CB dispersion, (b) and (b') 2# CB dispersion, (c) and (c') 3# CB dispersion, and (d) and (d') 4# CB dispersion.

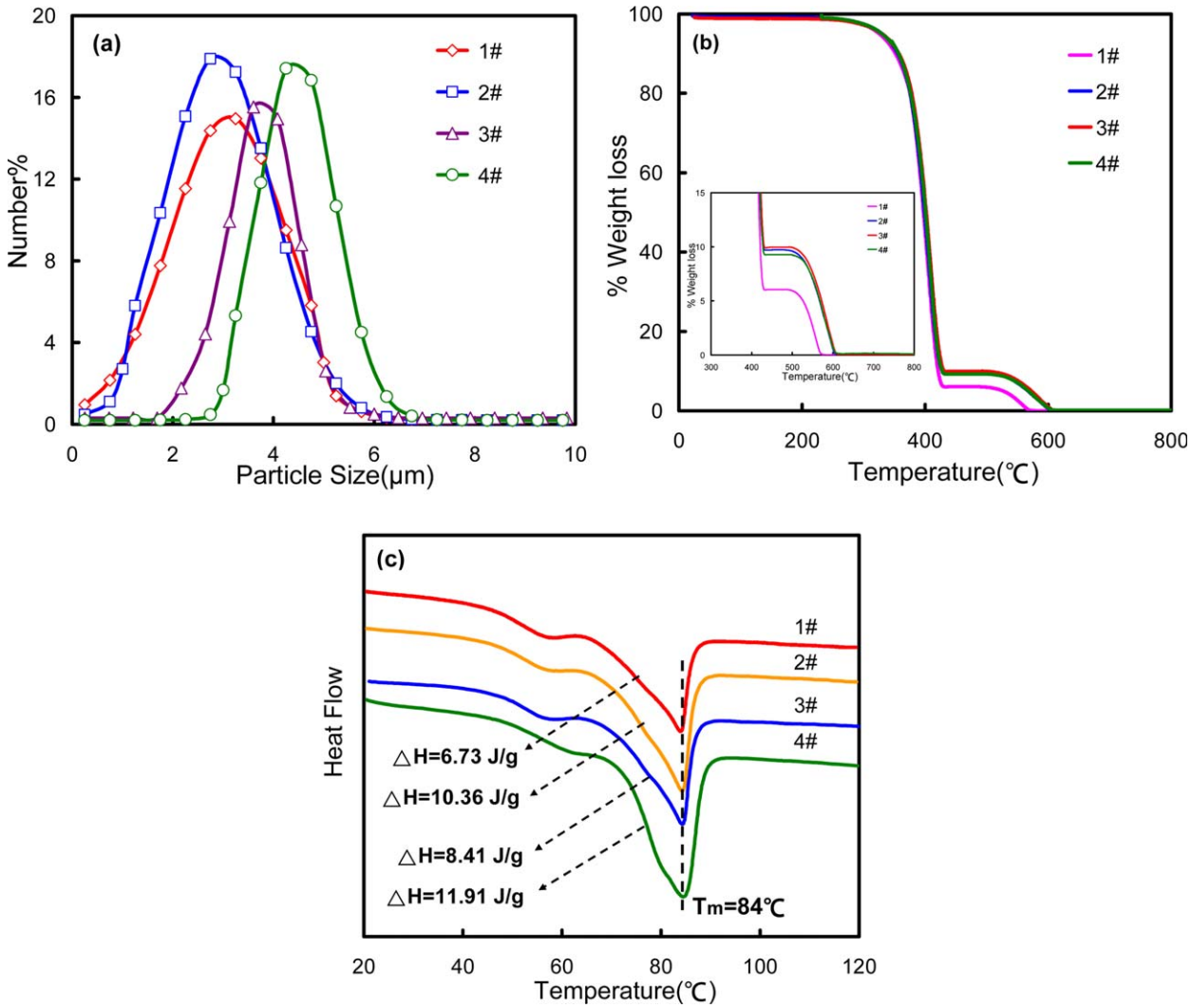

Figure 9. Particle size of the microspheres and content of every component in the microspheres, (a) the distribution of particle size of microspheres, (b) TGA curves of microspheres, and (c) DSC traces of microspheres. [Color figure can be viewed in the online issue, which is available at wileyonlinelibrary.com.]

Table III. Content of Every Component in the Microspheres

CB dispersion	Particle size of microsphere (μm)	Content of every component (%) in microsphere		
		CB	Wax	Resin
1#	3.12	6.03	4.73	89.24
2#	3.44	9.73	7.28	82.99
3#	3.99	9.96	5.96	84.08
4#	4.86	9.24	8.36	82.40

2# is more stable than Sample 1#, with a zeta potential of −45 mV at pH = 7 and a CCP of 2.2. The remarkably improved stability of Sample 2# could be attributed to the strong SO_4^- anion and π–π double bond in SE-10N, which is not influenced by pH. Meanwhile, the increase of number of ethylene oxide groups in SE-10N further improves the pH stability of CB dispersion with stronger steric stabilization than Sur-1.

CB encapsulation with PS through emulsion polymerization can enhance the stability of CB dispersion. As shown in Figure 7(b), comparison between Samples 3# and 4# indicates that zeta potential increases with increasing amount of polymer encapsulated on the CB surface, accordingly, CB pH stability improved. The CCP of these encapsulated CB dispersions further decreases to 2.0 for Sample 3# and 1.8 for Sample 4#.

Effect of pH Stability on Heterocoagulation Behavior

Our previous study showed that the coagulation efficiency of the three-component system (Resin–WP–CB) reached the peak value as the pH decreased to 2.0. As such, the heterocoagulation behavior was investigated at pH = 2.0 in the present study. As shown in Figure 8(a–d), microspheres prepared from the heterocoagulation of CB samples 1#–4# exhibit spherical forms with uniform dispersion, with an average particle size of 3.0–5.0 μm [Figure 9(a)].

CB distribution in the microspheres was studied using TEM, as shown in Figure 8(a'–d'). For microspheres using CB dispersion system 1#, only a small amount of CB is observed, and many CB particles aggregate around the microsphere surface. For CB dispersion system 2#, a large amount of CB particles are involved in the microspheres. However, many of these particles form big clusters, thereby decreasing the CCP to 2.0. For CB dispersion 3#, microspheres with high CB contents and uniform CB dispersion are obtained. When the CCP of the CB dispersion is 1.8 [Sample 4#, Figure 8(d')], the amount of CB involved in the microspheres is slightly lower than that in Sample 3# but maintained good dispersion. The TEM images evidently show that the stability of CB dispersion considerably affects the content and distribution of CB in the microspheres.

DSC and TGA were performed to quantify the amounts of WP and CB in the microspheres, with results shown in Figure 9(b,c) and data in Table III. The coagulated microspheres contain 10 wt % CB, 6.0 wt % WP, and 84.0 wt % Resin. The CB content reduces to 6.03 wt % for Sample 1#, whereas that of Samples 2#–4# exceed 9.0 wt %. These results are consistent with the TEM observations. Similar to the feed level of CB, the amount of CB in Sample 3# reaches 9.96 wt %. By contrast, the amount of WP changes when using different CB dispersions. Specifically, the amount of WP in Sample 1# is lower than that in Samples 2# and 4#. For Sample 3#, the amount of WP is the closest to the feed level.

The composition and CB distribution of the heterocoagulated microspheres changes depending on the stability of CB dispersions used. Generally, mixing of CB, WP, and Resin in aqueous media causes redistribution of free emulsifiers and dispersants in the mixture until a new balance is reached. CB particles without encapsulated PS exhibit weak interactions with the dispersants. Thus, although CB dispersion 2# presents a CCP of 2.2, which is similar to that of Resin and WP, a large amount of dispersants may peel off during dispersant rebalancing in the mixture, resulting in the formation of CB aggregates.

CB dispersion encapsulated with PS present different changes. Encapsulation of polymers on the CB surface can improve the affinity of dispersants on the surface. Furthermore, SE-10N, which was used in encapsulating polymerization, is a reactive dispersant. These factors can greatly reduce the possibility of dispersant redistribution during mixing, thereby facilitating the high coagulation efficiency of Sample 3#. Nevertheless, further research must be performed to investigate heterocoagulation kinetics by using different CCPs of each component.

CONCLUSIONS

Nanocomposite microspheres containing Resin, WP, and CB were prepared with desired CB dispersion through heterocoagulation. Three types of anionic dispersants with different lengths of nonionic chains and reactivity were used to disperse CB in aqueous medium. Finely dispersed CB was encapsulated with PS through emulsion polymerization to reduce the pH sensitivity of the dispersion. Reactive anionic dispersants with long nonionic chains providing steric stabilization and intensify charges as the literature[21,22] reported effectively decreased the CCP from 5.0 to 2.2. PS encapsulation on CB particles further decreased the CCP to 1.8. With increasing amount of polymer encapsulated on the CB surface, CB pH stability improved. A good encapsulation was performed with St/CB = 1/4 by using APS as the initiator. During heterocoagulation, PS-coated CB particles with a CCP of 2.0, similar to that of Resin and WP, tended to achieve fine dispersion and high content of CB in the microspheres. This finding could be due to the synergistic coagulating effect and solid adsorption of the dispersant on the CB surface. Nanocomposite microspheres with excellent dispersion and high content of pigment are expected to find application in high quality toner with increased homogeneity and outstanding print performance.

In the recipe, the theoretical content of CB, wax, and resin is 10 wt %, 6.0 wt %, and 84 wt %, respectively.

ACKNOWLEDGMENTS

This work was supported by grant from the National Natural Science Foundation of China (Grant 51373053).

REFERENCES

1. Du, X. M.; Li, T. L.; Li, L. J. *J. Mater. Chem. C* **2015**, *3*, 3545.
2. Kiatkamjornwong, S.; Pomsanam, P. *J. Appl. Polym. Sci.* **2003**, *89*, 238.
3. Farag, R.; Mohamed, N. H.; Elsaeed, S. M. *J. Dispersion Sci. Technol.* **2015**, *36*, 228.
4. Ataeefard, M. J. *Compos. Mater.* **2015**, *49*, 1553.
5. Liu, H. B.; Wen, S. G.; Wang, J. H.; Zhu, Y. *J. Appl. Polym. Sci.* **2012**, *123*, 3257.
6. Turner, A. J.; Nair, S.; Lai, Z.; Bhatia, S. R. *J. Appl. Polym. Sci.* **2011**, *122*, 1358.
7. Kim, S. Y.; Kim, B. Y.; Yon, K. Y. *J. Imaging. Sci. Technol.* **2013**, *57*, 503.
8. Zhang, Y. L.; Xv, C.; Guan, A. G.; Wu, G. Z. J. E. *China. Univ. Sci. Technol. Nat. Sci. Edi.* **2013**, *39*, 529.
9. Lee, Y. R.; Kim, S. C.; Lee, H.; Jeong, H. M.; Raghu, A. U.; Reddy, K. R.; Kim, B. K. *Macromol. Res.* **2011**, *19*, 68.
10. Eisermann, C.; Damm, B.; Winzer, B. *Powder. Technol.* **2014**, *253*, 338.
11. Jiang, D.; Wang, C. S.; Jiang, Z. L. *Chin. J. Process. Eng.* **2015**, *15*, 153.
12. Jada, A.; Ridaoui, H.; Vidal, L.; Donnet, J. B. *Colloids. Surf. A Physico. Chem. Eng. Aspects* **2014**, *458*, 190.
13. Hanaor, D.; Michelazzi, M.; Leonelli, C. *J. Eur. Ceram. Soc.* **2012**, *32*, 236.
14. Jacquot, F.; Logie, V.; Brilhac, J. F.; Gilot, P. *Carbon* **2002**, *40*, 335.
15. Li, H. Y.; Chen, H. Z.; Xv, W. J. *Colloids. Surf. A Physico. Chem. Eng. Aspects* **2005**, *254*, 173.
16. Tiarks, F.; Landfester, K.; Antonietti, M. *Macromol. Chem. Phys.* **2001**, *202*, 51.
17. Kang, S.; Jones, A. R.; Moore, J. S.; White, S. R.; Sottos, N. R. *Adv. Funct. Mater.* **2014**, *24*, 2948.
18. Reddy, K. R.; Sin, B. K.; Yoo, C. H.; Sohn, D.; Lee, Y. *J. Colloid Interface Sci.* **2009**, *340*, 160.
19. Hassan, M.; Reddy, K. R.; Haque, E.; Minett, A. I.; Gomes, V. G. *J. Colloid Interface Sci.* **2013**, *410*, 44.
20. Sis, H.; Birinci, M. *Colloids. Surf. A Physico. Chem. Eng. Aspects* **2009**, *341*, 60.
21. Wu, B. Y. *Appl. Technol. Market* **1995**, *10*, 11. (in Chinese)
22. Han, S. J.; Lee, H.; Jeong, H. M.; Kim, B. K.; Raghu, A. V.; Reddy, K. R. J. *Macromol. Sci. Part B: Phys.* **2014**, *53*, 1194.
23. Morris, E. A.; Weisenberger, M. C.; Bradley, S. B.; Abdallah, M. G.; Mecham, S. J.; Pisipati, P.; McGrath, J. E. *Polym.* **2014**, *55*, 6473.
24. Reddy, K. R.; Lee, K. P.; Gopalan, A. I.; Kim, M. S.; Showkat, A. M.; Nho, Y. C. J. *Polym. Sci. Part A: Polym. Chem.* **2006**, *44*, 3357.
25. Reddy, K. R.; Jeong, H. M.; Lee, Y.; Raghu, A. V. J. *Polym. Sci. Part A: Polym. Chem.* **2010**, *48*, 1478.
26. Papirer, E.; Lacroix, R.; Donnet, J. B. *Carbon* **1996**, *34*, 1521.
27. Darmstadt, H.; Roy, C. *Carbon* **2003**, *41*, 2653.
28. Casado, R. M.; Lovell, P. A.; Navabpour, P.; Stanford, J. L. *Polym.* **2007**, *48*, 2554.
29. Zhou, Y. Y.; Zhang, Q. Y.; Liu, Y. L. *Colloid. Polym. Sci.* **2013**, *291*, 2399.
30. Lelu, S.; Novat, C.; Graillat, C.; Guyot, A.; Lami, E. B. *Polym. Int.* **2003**, *52*, 545.
31. Fu, S. H.; Du, C. S.; Wang, C. X. *Colloids. Surf. A: Physico. Chem. Eng. Aspects* **2013**, *428*, 2.
32. Wang, C. X.; Zhang, X.; Lv, F. B.; Peng, L. Y. *J. Appl. Polym. Sci.* **2012**, *124*, 5194.